





Efficient Low-Complexity Optimized Channel Estimating Methods for OFDM-Based Low-Voltage Broadband Power Line Communication Systems

Evans Wilson Akpari¹ , Solomon Nunoo² , Faith Kwaku Deynu¹ ,
Michael Wellington Apprey¹ 

¹Electrical and Electronic Engineering Department, Ho Technical University, P. O. Box HP 217, Ho, Ghana,
eakpari@htu.edu.gh, fdeynu@htu.edu.gh, mapprey@htu.edu.gh

²Department of Electrical and Electronic Engineering, University of Mines and Technology, P. O. Box 237,
Tarkwa, Ghana, snunoo@umat.edu.gh

Abstract— Broadband Power Line Communication (BB-PLC) technology enables data transmission for smart grid applications. Nevertheless, channel equalizers are required in the receiver to estimate and compensate for the nonlinear time-variant impulse response and noise interference effects introduced by the BB-PLC channel. In this paper, we append the Particle Swarm Optimization (PSO) algorithm and its proposed improved version to the commonly used Least-Square (LS) and Linear Minimum Mean Square Error (LMMSE) algorithms to advance four new block-type pilot-aided hybrid channel estimation algorithms for low-voltage Orthogonal Frequency Division Multiplexing (OFDM)-based BB-PLC systems. Extensive numerical simulation results for four different M-QAM formats ($M = 8, 16, 32, 64$) show that the proposed algorithms significantly improve the performance of the traditional LS and LMMSE estimators, at least for the parameters of the BB-PLC system studied in this work. In addition, the computational load complexity of the PSO-inspired LMMSE algorithm is lower compared to the conventional LMMSE estimator.

Index Terms— Low-Voltage Broadband PLC, improved PSO, LS, LMMSE, Channel Estimation, OFDM-based M-ary Quadrature Amplitude Modulation (M-QAM)

I. INTRODUCTION

Recently, Power Line Communication (PLC) technology is receiving a great deal of research attention due to its ability to support high-speed data transmission for many emerging applications such as the Internet of Things (IoT), smart grids, cities, telemetry, homes, industries, etc [1]. Based on the commonly used bandwidth criterion, PLC technologies can be put into three different categories of Ultra-Narrowband PLC (UNB-PLC, < 3 kHz frequency), Narrowband PLC (NB-PLC, 3 kHz \leq frequency ≤ 500 kHz) and Broadband PLC (BB-PLC, 1 MHz \leq frequency ≤ 250 MHz) [1]. As a through-the-grid communication technology, each of these categories can be used for transmission of low and high data rate applications based on single- and multi-carrier modulation techniques in low,

medium and high voltage sections of existing installed power transmission and delivery infrastructure. However, due to the diversity of practical power network configurations and fluctuations of various loads connected to the termination points of the networks, PLC channels experience time-varying and multipath propagation frequency-selective fading, signal attenuation, reflection, and strong noise interference effects, which can significantly degrade system performance. To provide robust immunity against the frequency-selective multipath fading effects, multi-carrier OFDM-based on single-carrier Quadrature Amplitude Modulation (QAM) formats have become the preferred solution over the last decade [2]. In this case, the OFDM modulation technique transforms the frequency-selective fading effects into flat-fading effects and also supports higher data rates in PLC systems. Beyond this, channel equalization algorithms are required in PLC receivers to estimate and remove the inevitable unknown frequency impulse response and noise interference effects introduced by the PLC channel to retrieve the transmitted data with the minimum level of bit errors [3]. It is worth mentioning here that the noise interference effects are pronounced at low frequencies.

For this reason, a plethora of channel estimation methods have been published in the literature for OFDM-based PLC channels which can generally be put into two main categories: 1) pilot-aided [4][5], e.g., Least Square (LS) [6], Particle Swarm Optimization (PSO) [6], Maximum-Likelihood (ML)[8] complementary sequences[2], Linear Minimum Mean Square Error (LMMSE) [9], Compressed Sensing-based Orthogonal Matching Pursuit (CS-OMP)[10], Zadeh-based Minimum Mean Square Error (Z-MMSE) [11], adaptive trimmed/weighted LS [13], particle filtering [12], etc., and 2) blind, e.g., Least-Mean-Square (LMS)[13], adaptive Maximum a-Posteriori (MAP) [14], etc. Other researchers proposed modulation techniques that are tailored to be resilient to the noise interference effects of the PLC channels[15] in conjunction with traditional channel estimation methods. Among these channel estimators, the LS [6] and LMMSE [9] are the most commonly used methods. Although these channel estimation techniques reported improved results for OFDM-based BB-PLC channels, the reported results are suboptimal [6]. This is because the traditional LS and LMMSE channel estimators may lose optimality in the presence of noise (e.g., impulsive noise), especially when the noise deviates from the Gaussian distribution. Particularly, while the LS is simple, its main drawback is poor noise rejection. The LMMSE on the other hand has good rejection for noise but at the expense of high computational complexity. For the implementation of channel estimation and equalization in real-time PLC systems, computational complexity issues should be considered. Furthermore, the characteristics of the time-varying channel impulse response and noise interference effects require an optimal channel estimator in PLC systems. Therefore, the work in this paper seeks to fill this performance deficiency of the LS and LMMSE channel estimation methods for PLC systems, since this has not been investigated previously, to the best of our knowledge.

In this paper, we contribute to the following:

- We applied the PSO algorithm to advance four new channel estimators based on the basic LS and LMMSE algorithms for low-voltage OFDM-based BB-PLC systems. In the proposed algorithms, the PSO algorithm is applied to optimize the performance of the LS and LMMSE estimators.
- Beneficially, while the proposed PSO-inspired LS technique improves the noise rejection capability of the basic LS algorithm, the PSO-based LMMSE technique lowers the computational complexity of the traditional LMMSE algorithm.
- Results of extensive numerical simulations conducted for four different M-QAM formats ($M = 8, 16, 32, 64$) showed that our proposed algorithms offer relatively better performance, compared to the traditional implementation of LS and LMMSE algorithms, at least for the system parameters studied in this work.

The rest of the paper is organised as follows: Section 2 presents the system model of the low-voltage BB-PLC system. Section 3 presents the theoretical background of the proposed LS and LMMSE channel estimation techniques based on the IPSO algorithm, including its complexity analysis. Section 4 describes the simulation conducted to evaluate the performance of the proposed algorithms, including commentary on the results. Discussion of the performance of the proposed algorithms vis-à-vis related works is carried out in Section 5, while Section 6 concludes the paper.

II. SYSTEM MODEL

Power-line channels exhibit different channel characteristics at different moments under multipath propagation, time-varying loads, attenuation and strong noise interference effects. Since the work in this paper concerns estimating the BB-PLC channel, in this section, we briefly describe the characteristics of the channel including the noise model adopted. The system model used is based on the typical OFDM-based low voltage (LV) BB-PLC system shown in Fig. 1 (a), which consists of a transmitter, PLC channel and receiver [16].

A. Characteristics of LV BB-PLC channel

Typically, network topology consisting of NAYY150 and NAYY35 cables with characteristic impedances of 45Ω and 70Ω respectively are considered for LV power lines that provide smart metering applications. While NAYY150 cables serve as the main distribution power lines from the utility provider to the customer's premises, NAYY35 cables are used for the connections within the premises. The typical geometric and electromagnetic parameters of NAYY150 and NAYY35 cables respectively can be found in [17]. As signals propagate over the power lines, they are affected by attenuation, which increases with the frequency and length of the line. This can be described by the multipath model for complex frequency response of a (0 – 30) MHz BB-PLC channel as [17]:

$$H(f) = \sum_{i=1}^N \underbrace{g_i}_{\text{Weighting factor}} \cdot \underbrace{\exp\left[-\left(a_0 + a_1 f^k\right) d_i\right]}_{\text{Attenuation portion}} \cdot \underbrace{\exp\left[-j2\pi f \left(d_i/v_P\right)\right]}_{\text{Delay portion}} \quad (1)$$

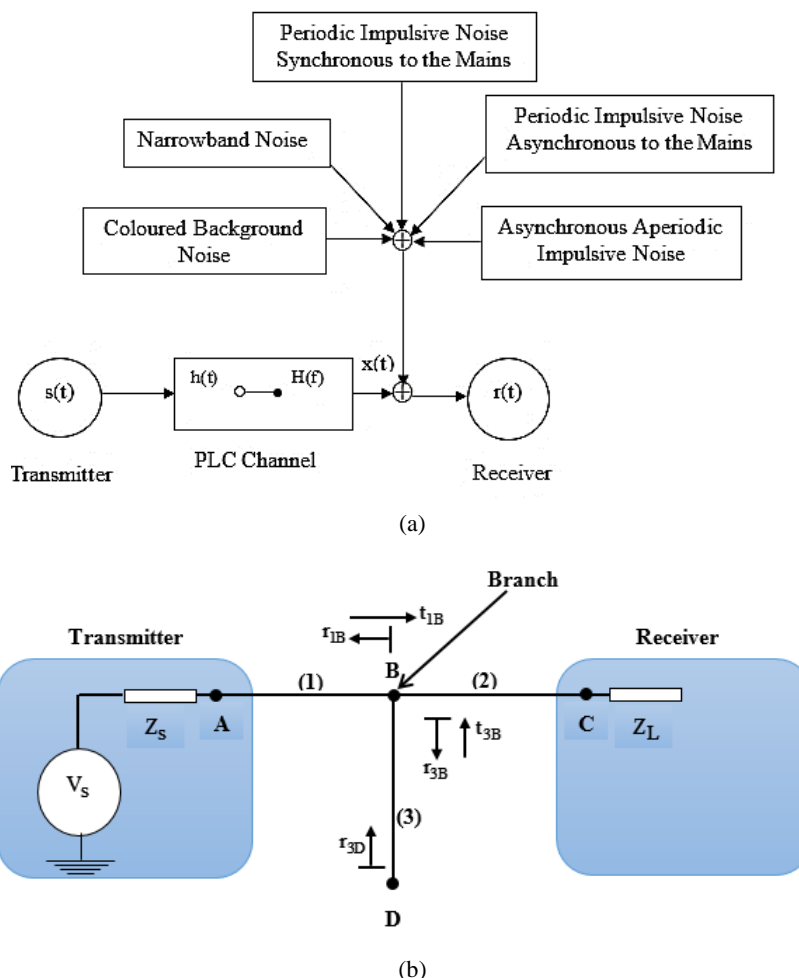


Fig. 1. System model: (a) A typical BB-PLC system [16] (b) Multipath signal propagation; cable with one branch [17].

To explain the terms in (1) [17], we use the simple distribution network topology shown in Fig. 1 (b) for signal propagation over a BB-PLC system. AC is the length of the power line between the transmitter and receiver with source and load impedances of Z_s and Z_L respectively. BD is the branch length, with point B considered the centre of AC. The transmitter and receiver are impedance-matched, i.e., the impedance of the length between the transmitter and branch point B (Z_{L1}) is equal to the impedance of the length between branch point B and the receiver (Z_{L2}). The weighting factor g_i in (1) [17] is a product of reflection and transmission factors, which are assigned to each path i was taken by a signal. From Fig. 1 (b), the reflection factors are given as [17], [18]:

$$r_{1B} = \frac{\frac{Z_{L2}Z_{L3}}{Z_{L2}+Z_{L3}} - Z_{L1}}{\frac{Z_{L2}Z_{L3}}{Z_{L2}+Z_{L3}} + Z_{L1}} = \frac{Z_{L2}Z_{L3} - Z_{L1}(Z_{L2} + Z_{L3})}{Z_{L2}Z_{L3} + Z_{L1}(Z_{L2} + Z_{L3})} \quad (2)$$

$$r_{3D} = \frac{Z_D - Z_{L1}}{Z_D + Z_{L1}} \quad (3)$$

$$r_{3B} = \frac{\frac{Z_{L1}Z_{L2}}{Z_{L1}+Z_{L2}} - Z_{L3}}{\frac{Z_{L1}Z_{L2}}{Z_{L1}+Z_{L2}} + Z_{L3}} = \frac{Z_{L1}Z_{L2} - Z_{L3}(Z_{L1}+Z_{L2})}{Z_{L1}Z_{L2} + Z_{L3}(Z_{L1}+Z_{L2})} \quad (4)$$

Similarly, the transmission factors can be expressed as [17], [18]:

$$t_{1B} = 1 - |r_{1B}| \quad (5)$$

$$t_{3B} = 1 - |r_{3B}| \quad (6)$$

It is worthy to mention here that the weighting factor depends on the rate of occurrence of reflections and transmissions along given path i , so the more the frequency of occurrence, the smaller the weighting factor. Since the values of reflection and transmission factors for a power line are always less than or equal to 1, the weighting factor g_i is consequently also less than or equal to 1 ($g_i \leq 1$). Table I shows how to calculate the weighting factor g_i for the path length i (d_i) with N-paths. The second term in (1) [17] deals with the effect of attenuation on data transmitted through the BB-PLC channel, which is a function of both cable length (d_i) and transmission frequency (f). The exponent k is the attenuation factor, usually between 0.5 and 1. The parameters a_0 and a_1 represent the approximated attenuation constants of the power line cable for BB-PLC. The last term in (1) [17], characterize the delay experienced by data transmitted over the power line due to the multipath effect of the channel, where v_p is the speed of propagation in the power line conductor [17].

TABLE I. POSSIBLE SIGNAL PROPAGATION PATHS FROM TRANSMITTER TO RECIEVER [17]

Path No.	Pathway	g_i	d_i
1	A→B→C	t_{1B}	L_1+L_2
2	A→B→D→B→C	$t_{1B} r_{3D} t_{3B}$	$L_1+2L_3+L_2$
.	.	.	.
N	A→B→(D→B) ^{N-1} →C	$t_{1B} r_{3D}(r_{3B} r_{3D})^{N-2} t_{3B}$	$L_1+2(N-1)L_3+L_2$

To investigate the transmission behaviour of the power line modelled in (1), we simulated a signal propagated over a BB-PLC system based on Fig. 1 (b). The following parameters: $Z_A=Z_{L1}=Z_C=Z_{L2} = 45 \Omega$, $Z_D=0 \Omega$ (where Z_A , Z_C and Z_D are the impedances at points A, C and D respectively) and $Z_{L3} = 70\Omega$ (Z_{L3} is the impedance of line BD) used in the simulation were obtained from [17]. The load connected on branch BD of length 50 m has a different impedance than the impedance of the direct line length AC which results in reflection with factors as given previously. In the simulation, the length of AC is varied between 100 m to 500 m. In Fig. 2, we plotted results of the behaviour of the BB-PLC channel with frequency selective fading effects based on simulation of (1) at different lengths of AC. In this case, the number of the path is one. As can be observed from Fig. 2, the notches shown in the frequency response illustrate the effects of frequency selective fading of the BB-PLC

channel. Thus, the impedance exhibits a clear time-variation with deference to the mains that is indeed frequency selective, i.e. different kinds of variations occur at different bands.

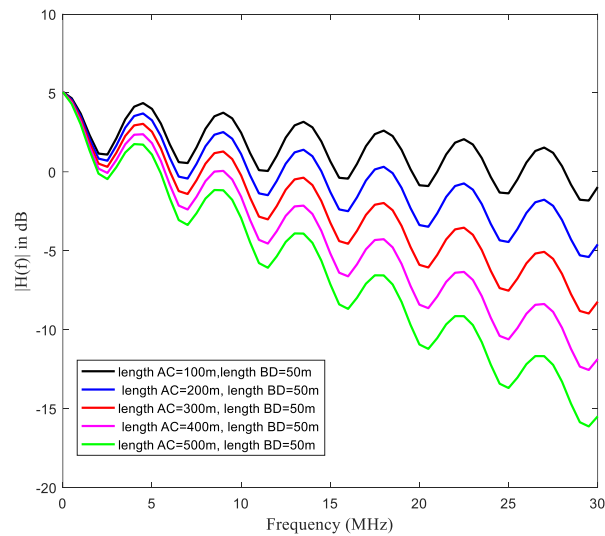


Fig. 2. Behaviour of BB-PLC channel due to frequency selective fading.

For this reason, a multicarrier modulation technique such as OFDM is preferred for data transmission to provide immunity against the frequency selective fading and severe noise interference effects presented by the BB-PLC channels [17]. From Fig. 2, it can be seen that the spreading of the frequency notches occurs in an interval of 5 MHz, which means that each sub-carrier would be required to have a maximum bandwidth of approximately 5 MHz to ensure flat frequency fading of the BB-PLC channel is within a frequency range of 0-30 MHz, as considered in this paper. To verify the multipath characteristics of the LV BB-PLC channel, in Fig. 3, we obtained simulation results based on (1) for four propagation paths, using the parameters in [17] listed in Table II.

TABLE II. LIST OF PARAMETERS FOR FOUR-PATH BB-PLC CHANNEL MODEL [17]

Attenuation Parameters				
$k=1, a_1 = 0, \alpha_1 = 7.8 \times 10^{-10}$ (s/m), $v = 3.0 \times 10^8$ (m/s)				
Path Parameters				
i	1	2	3	4
g_i	0.64	0.38	-0.15	0.05
d_i (m)	200	222.4	244.8	267.5

As shown in Fig. 3, when the transmitted data takes four paths through the LV BB-PLC channel, only a few notches can be observed in the frequency response for both magnitude and phase response. Similarly, in Fig. 4, we obtained the multipath characteristics of the LV BB-PLC channel with fifteen paths using the parameters given in Table III [17]. However, as shown in Fig. 4, when the number of propagation paths is increased from 4 to 15, the position of the notches changes with the frequency of

the magnitude and phase responses. As illustrated in Fig. 3, the attenuation of notched points and signal distortion tend to increase.

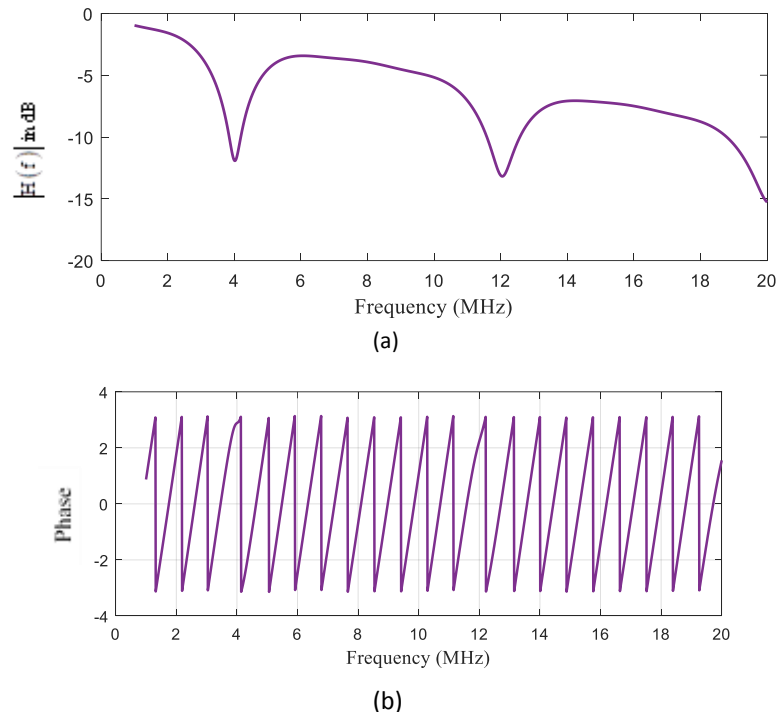


Fig. 3. Multipath characteristics of the LV BB-PLC channel with 4 paths in terms of (a) magnitude and (b) phase.

TABLE III. LIST OF PARAMETERS FOR FIFTEEN-PATH BB-PLC CHANNEL MODEL [17]

Attenuation Parameters					
$k=1, a_1 = 0, \alpha_1 = 7.8 \times 10^{-10}$ (s/m), $v = 3.0 \times 10^8$ (m/s)					
Path Parameters					
i	g_i	d_i(m)	i	g_i	d_i(m)
1	0.029	90	9	0.071	411
2	0.043	120	10	-0.035	490
3	0.103	113	11	0.065	567
4	-0.058	143	12	-0.055	740
5	-0.045	148	13	0.042	960
6	-0.040	200	14	-0.059	1130
7	0.038	260	15	0.049	1250
8	-0.038	322			

In this context, with an increasing number of propagation paths for signal reception, it is justifiable that there will be an increased probability of receiving a distorted signal. Hence, Figs. 3 and 4 confirm the prediction of (1) in [17] that a BB-PLC channel behaves perfectly as a multipath channel, in which case a signal propagated from the transmitter can spread into an infinite number of possible paths before it reaches the receiver.

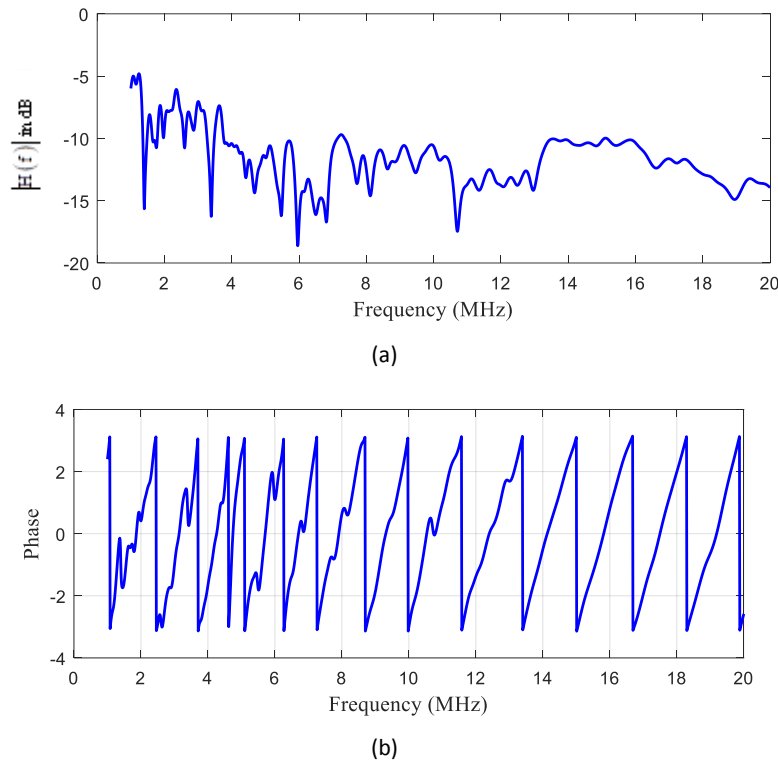


Fig. 4. Multipath characteristics of the LV BB-PLC channel with 15 paths in terms of (a) magnitude and (b) phase.

B. Noise characteristics of LV BB-PLC channel

The noise in BB-PLC channels constitutes vital constraints that define the nature of interferences in PLC systems. As shown in Fig. 1 (a), the noise interference scenario in a typical power line channel can be put into three categories of background, narrowband and impulsive noise effects [19][20], which add up to the propagated signal by the channel during data transmission. These noises usually cause disturbances within a frequency range of 0-100 MHz, which falls within the frequency range of the LV BB-PLC channel considered in this paper. The background noise has low signal power, and its Power Spectral Density (PSD), $S_b(f)$ in dBm/Hz, is modelled as a first-order exponential given by[19][20]:

$$S_b(f) = N_o + N_1 \ell^{-f/f_1} \quad (7)$$

where, N_o = constant noise power density, f = considered frequency band (0-30 MHz)

N_1 and f_1 = parameters of the exponential function.

The PSD of a narrowband noise, $S_n(f)$, is modelled as a parametric Gaussian function given by[19][20]:

$$S_n(f) = \sum_{k=1}^N A_k \cdot \ell^{-\left[\frac{(f-f_{o,k})}{2B_k}\right]^2} \quad (8)$$

where, A_k = amplitude of the kth narrowband signal, $f_{o,k}$ = centre frequency, B_k = bandwidth,

N = narrowband interferences.

Impulsive noise, which has short intervals with high spectral power, and hence proves to be a major contributor to erroneous data transmission over power lines can be modelled according to the IEEE 1901 standard as[19][20]:

$$p(t) = (u(t) - u(t - T_d)) \cdot \sum_{i=0}^{N_d-1} A_i e^{-\alpha_1 |t|} e^{-j2\pi f_i t} \quad (9)$$

where $p(t)$ is the time-domain impulse noise, $u(t)$ denotes the unit step function, N_d represents the number of damped sinusoids in an impulse, A is the impulse amplitude, T_d is the impulse duration, α_1 is the damping factor and f_i denotes the pseudo frequency of the sinusoids

All these noises are added together in (10) to get the overall BB-PLC channel noise which perturbs the time-domain data signals.

$$\text{BB - PLC Channel Noise} = S_b(f) + S_n(f) + p(t) \quad (10)$$

To illustrate their net effect, in Fig. 5, we obtained via simulation the PSD of the overall noise in the BB-PLC channel using the parameters given in Table IV. From Fig. 5, the PSD function shows that the noise power of the BB-PLC channel increases with increasing bandwidth (0-30 MHz).

TABLE IV. BB-PLC CHANNEL NOISE SIMULATION PARAMETERS

Parameters	Specifications
Channel type	BB-PLC multipath channel
PLC Frequency Range(MHz)	0-30
FFT size	64
Sampling Frequency (MHz)	320
Sub-carrier Spacing (MHz)	5
Mains Frequency (Hz)	50/60

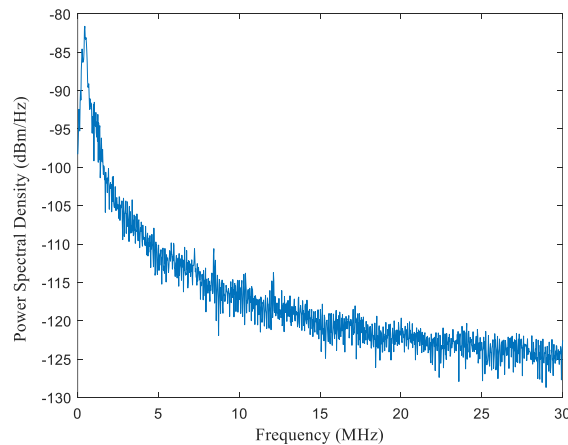


Fig. 5. PSD of the overall noise in a typical BB-PLC channel.

At 5 MHz bandwidth, the noise power is approximately -112 dBm and increases to -125 dBm at 10 MHz. In this case, increasing a communication system's bandwidth to allow for the transmission of more data, means there is a greater tendency of enhancing the noise power in the system, which may theoretically reduce the dynamic range of the system. This will require a major trade-off in all communication systems including the OFDM-based BB-PLC channel considered in this paper. Hence, the removal of noise in BB-PLC channels is very vital to preserving the quality of the data detected by the OFDM receiver.

III. BB-PLC CHANNEL ESTIMATION ALGORITHMS

As the received time-domain signal is impaired by unknown time-varying impulse responses and noises of BB-PLC channels, channel estimation is crucial for receivers to recover the transmitted signal in PLC systems. As stated previously, the LS [6] [11], [13] and LMMSE [9] are indisputably the most commonly used channel estimation algorithms for OFDM-based PLC systems. In addition, the PSO algorithm can be applied for effective and efficient channel estimation in PLC systems [6]. Therefore, in this section, we describe these algorithms, which are fundamental to our proposed channel estimation algorithms used in this work. In this work, we consider the transmission of OFDM signals over a BB-PLC system based on Fig. 1 (a) [16]. At the receiver side, the received data signal \mathbf{Y} can be expressed as [9]:

$$\mathbf{Y} = \mathbf{X}\mathbf{H} + \mathbf{Z} \quad (11)$$

$$\text{where, } \mathbf{X} = \begin{bmatrix} \mathbf{X}[0] & \mathbf{0} & \dots & \mathbf{0} \\ \mathbf{0} & \mathbf{X}[1] & & \vdots \\ \vdots & & \ddots & \mathbf{0} \\ \mathbf{0} & \dots & \mathbf{0} & \mathbf{X}[N-1] \end{bmatrix}, \mathbf{Y} = \begin{bmatrix} \mathbf{Y}[0] \\ \mathbf{Y}[1] \\ \vdots \\ \mathbf{Y}[N-1] \end{bmatrix}, \mathbf{H} = \begin{bmatrix} \mathbf{H}[0] \\ \mathbf{H}[1] \\ \vdots \\ \mathbf{H}[N-1] \end{bmatrix}, \mathbf{Z} = \begin{bmatrix} \mathbf{Z}[0] \\ \mathbf{Z}[1] \\ \vdots \\ \mathbf{Z}[N-1] \end{bmatrix}$$

\mathbf{X} and \mathbf{Y} represent the transmitted and received data vectors respectively, \mathbf{H} and \mathbf{Z} denote the impulse response and noise vectors respectively of the BB- PLC channel. Estimation of PLC channels can be achieved by using either known signal overheads (i.e., pilot symbols) or received symbols (i.e., blind estimation). Due to the fast-varying fading nature of BB-PLC channels and the availability of pilot symbols in OFDM-based PLC systems, the work in this paper adopts the pilot-aided channel estimation method. Therefore, similar to (11), the received pilot matrix can be expressed as:

$$\mathbf{Y}_p = \mathbf{X}_p \mathbf{H}_p + \mathbf{Z}_p \quad (12)$$

A. LS algorithm

The LS estimation method forms the basis of many other channel estimation algorithms and consists of the multiplication of the received pilot data block by the inverse of the transmitted pilot data block. In this case, channel estimation for each sub-carrier of OFDM based on the LS algorithm can be expressed as [9]:

$$\hat{\mathbf{H}}_{\text{LS}}[k] = \frac{\mathbf{Y}_p[k]}{\mathbf{X}_p[k]} = \mathbf{X}_p^{-1} \mathbf{Y}_p = \begin{bmatrix} \mathbf{y}_0 & \mathbf{y}_1 & \dots & \mathbf{y}_{N-1} \\ \mathbf{x}_0 & \mathbf{x}_1 & \dots & \mathbf{x}_{N-1} \end{bmatrix} = \mathbf{H}_p[k] + \frac{\mathbf{Z}_p[k]}{\mathbf{X}_p[k]} \quad (13)$$

In (13), \mathbf{X}_p and \mathbf{Y}_p are the matrices representing the transmitted and received pilot symbols respectively, \mathbf{H}_p denotes the matrix for the channel response of the pilot subcarriers, N is the total number of pilot subcarriers and \mathbf{Z}_p denotes the noise experienced by the pilot subcarriers. From (13), it can be seen that LS channel estimation is obtained by performing only element by element division of complex vectors, which makes its implementation complexity quite simple. However, the LS is very sensitive and vulnerable to noise distortion effects, which can limit its performance in practical BB-PLC systems. This drawback can best be described by the MSE of the LS estimation, which is expressed as [9]:

$$\begin{aligned} \text{MSE}_{\text{LS}} &= \mathbb{E} \left\{ \left(\mathbf{H} - \hat{\mathbf{H}}_{\text{LS}} \right)^H \left(\mathbf{H} - \hat{\mathbf{H}}_{\text{LS}} \right) \right\} = \mathbb{E} \left\{ \left(\mathbf{H} - \mathbf{X}^{-1} \mathbf{Y} \right)^H \left(\mathbf{H} - \mathbf{X}^{-1} \mathbf{Y} \right) \right\} \\ &= \mathbb{E} \left\{ \left(\mathbf{X}^{-1} \mathbf{Z} \right)^H \left(\mathbf{X}^{-1} \mathbf{Z} \right) \right\} = \mathbb{E} \left\{ \mathbf{Z}^H \left(\mathbf{X} \mathbf{X}^H \right)^{-1} \mathbf{Z} \right\} = \frac{\sigma_z^2}{\sigma_x^2} \end{aligned} \quad (14)$$

It can be deduced from (13) that the MSE of the LS estimator is inversely proportional to the channel SNR, and suggests that the LS estimator may suffer from noise distortion in PLC systems when the SNR is increased to improve signal quality. In this context, the simple low-complexity LS channel estimator is a poor rejecter of noise, since the noise samples still appear in (13), and hence require performance improvement. For this reason, a robust cost function is introduced in [19] that can suppress impulsive noise by weighting to improve the performance of the LS algorithm but its complexity is increased.

B. LMMSE algorithm

To overcome the limitation of the LS channel estimation method in the presence of noise, the LMMSE channel estimation method is introduced, which is an optimal channel estimator in the sense of the MSE. It involves the autocorrelation matrix of the channel in the frequency domain and is based on the more efficient MMSE technique, which is to minimise the MSE between the actual channel response \mathbf{H} and LS estimated channel response \mathbf{H}_{LS} . Using a weight matrix \mathbf{W} to define $\hat{\mathbf{H}}$ as $\mathbf{W}\tilde{\mathbf{H}}$ which corresponds to the MMSE estimate, the LMMSE estimator is given as [9]:

$$\hat{\mathbf{H}} = \mathbf{H}_{\text{LMMSE}} = \mathbf{W}\tilde{\mathbf{H}} = \mathbf{R}_{\mathbf{H}\tilde{\mathbf{H}}} \mathbf{R}_{\tilde{\mathbf{H}}\tilde{\mathbf{H}}}^{-1} \tilde{\mathbf{H}}$$

$$\begin{aligned}
 &= \mathbf{R}_{\mathbf{H}\tilde{\mathbf{H}}} \left(\mathbf{R}_{\mathbf{H}\mathbf{H}} + \frac{\sigma_z^2}{\sigma_x^2} \mathbf{I} \right)^{-1} \tilde{\mathbf{H}} \\
 &\approx \mathbf{R}_{\mathbf{H}\tilde{\mathbf{H}}} \left(\mathbf{R}_{\mathbf{H}\mathbf{H}} + \frac{\beta}{\text{SNR}} \mathbf{I} \right)^{-1} \tilde{\mathbf{H}}
 \end{aligned} \tag{15}$$

$$\mathbf{H}_{\text{LMMSE}} = \mathbf{R}_{\mathbf{H}\mathbf{H}} \left(\mathbf{R}_{\mathbf{H}\mathbf{H}} + \frac{\beta}{\text{SNR}} \mathbf{I} \right)^{-1} \mathbf{H}_{\text{LS}} \tag{16}$$

where $\mathbf{R}_{\mathbf{H}\mathbf{H}}$ denotes the channel autocorrelation matrix at pilot sub-carriers, β denotes the scaling or constellation factor, which depends on the modulation type. For QPSK, its value is 1; for 16-QAM being employed in this paper, its value is 17/9, where SNR is supposed to be known or accurately estimated, $\mathbf{I} = N_p \times N_p$ is the identity matrix and \mathbf{H}_{LS} is the vector containing the LS estimated samples of the channel frequency response given by (13). The MSE of the LMMSE channel estimator is given by [9]:

$$\text{MSE}_{\text{LMMSE}} = \mathbf{E} \left\{ \left(\mathbf{H} - \mathbf{H}_{\text{LMMSE}} \right)^{\mathbf{H}} \left(\mathbf{H} - \mathbf{H}_{\text{LMMSE}} \right) \right\} \tag{17}$$

Thus, (17) minimises the error between the actual channel response \mathbf{H} and the LMMSE estimated channel response $\mathbf{H}_{\text{LMMSE}}$. It is worth mentioning that the MSE of the LMMSE estimator also represents the error covariance matrix, and the optimal LMMSE estimator is its posteriori expectation. Nevertheless, the drawbacks of the traditional LMMSE technique are pretty obvious in (17), as it requires prior knowledge of channel LS estimate and SNR information at pilot sub-carriers, which are time-varying and always unknown in advance in actual systems. In addition, the LMMSE estimator requires matrix inversion every time the input data changes, which increases its computational complexity considerably. Consequently, the high complexity and high dependence on channel characteristics make the LMMSE estimator challenging to implement in real-time OFDM-based BB-PLC systems. In this context, a better LMMSE algorithm with reduced complexity is required.

C. PSO or Improved PSO (IPSO) algorithm

The basic PSO algorithm has first been applied for blind channel estimation in PLC systems with time-varying and frequency-selective channel response impaired by impulsive noise [6], besides its application for distribution state estimation [22], parameter identification and minimization of power losses [23] in power distribution networks. Assuming a stationary channel, the received values of transmitted M-QAM OFDM symbols at a given subcarrier, i may belong to one of M possible symbols which is considered a particle in the PSO algorithm. Thus, for the PSO algorithm, the particles constitute the swarm, also known as the population moves in a predefined search space. The PSO is a simple robust heuristic algorithm with low memory requirements that achieves fast convergence by using position and velocity update equations to iteratively search for the global

minimum (i.e., global optimal value) for the problem under study. That is, the main principle behind the PSO algorithm is to search the position of each particle in the search space, which represents the best estimation by the channel equalizer in this work. For each iteration, the velocity and position of each particle are updated respectively by [24]:

$$V(i) = \omega \times V(i) + c_1 \times \text{rand}(\) \times (P_{\text{best}}(i) - X(i)) + c_2 \times \text{rand}(\) \times (G_{\text{best}}(i) - X(i)) \quad (18)$$

$$x_{i+1} = x_i + V_{i+1} \quad (19)$$

where ω is the inertia weight factor which controls the change of velocity between successive iterations with values between 0.4 and 0.9, $V(i)$ denotes the particle velocity given as the rate of change of the next position with respect to x_i , the current position of the particle, $\text{rand}(\)$ is the random number between 0 and 1, $P_{\text{best}}(i)$ represents the local best particle that results in a minimum value of the cost function, $G_{\text{best}}(i)$ is the global best particle of the swarm which is the best value among all local best, c_1 and c_2 are the learning factors or acceleration constants (i.e., the rates at which local and global optima are achieved). The two extreme values, local best and global best, represent the optimal solution for local and global populations respectively. The PSO algorithm is terminated when the global minimum (or maximum) is attained after a predefined number of iterations.

Despite its advantages, the basic PSO algorithm has deficiencies in balancing the global best and local best of the population, which may cause the optimal solution to end in the local best when the population lacks diversity [24]. On the other hand, the inertia weight affects the local and global searching ability of the PSO algorithm, a larger value of the inertia weight means a larger particle velocity and vice versa. In this case, an efficient PSO algorithm can be derived by using a variable or adaptive inertia weight, instead of the constant inertia weight assumed in (18). Here, the inertia weight is updated based on the error value, which will eventually result in high speed and efficiency. Therefore, to improve the performance of the standard PSO algorithm in this paper, we proposed to use adaptive inertia weight defined by (20) [24]. With an update, the initial inertia weight ω assigned is replaced by the adaptive inertia weight $\omega_i(k)$ in (18) with (19) correspondingly updated.

$$\omega_i(k) = 0.5 \times \text{rand}(\) + \frac{\text{fitness}(g_{\text{best}})(k)}{\text{fitness}(P_{\text{best}})_i(k)} \quad (20)$$

where $\omega_i(k)$ is the adaptive inertia weight of the i^{th} particle at the k^{th} iteration, $\text{fitness}(g_{\text{best}})(k)$ denotes the global optimal fitness at k^{th} iteration, $\text{fitness}(P_{\text{best}})_i(k)$ is the optimal fitness of the i^{th} particle and $\frac{\text{fitness}(g_{\text{best}})(k)}{\text{fitness}(P_{\text{best}})_i(k)}$ is the range of [0, 1].

In terms of contribution by the new IPSO algorithm in this paper, the use of inertia weight adjustment based on the optimal fitness value of individual particles increases the diversity of the inertia weights and ensures a proper balance between the global best and local best. In addition, the mutation threshold for the particles corrects the imprecision of random mutation and thus, increases the diversity of the population effectively, since random solutions of population size, inertia weight and acceleration factors are initially assigned to the particles in the search space for the PSO algorithm.

D. Proposed optimized LS and LMMSE algorithms based on the improved PSO

Another disadvantage of the PSO algorithm is its vulnerability to local minima, where the particles become stagnant due to a lack of finer search capabilities in the algorithm. In this context, a hybrid of IPSO and the LS and LMMSE algorithms looks attractive to solve the local minima issue as well as overcome the main drawbacks of the conventional LS and LMMSE algorithms. Meanwhile, the PSO is shown to significantly outperform the conventional LS algorithm in [6]. Therefore, a channel estimation method that combines the conventional LS and IPSO algorithm with several iterations would give a better channel estimate. For these reasons, this paper makes use of the IPSO (or PSO) algorithm to advance two new channel estimation algorithms, i.e., IPSO-based LS and LMMSE estimators, for BB-PLC systems.

The proposed channel estimators apply the IPSO (or PSO) algorithm to optimize estimates by the LS and LMMSE channel equalizers and obtain the best channel and fitness value defined by a cost function and thus, minimise high channel MSE due to multipath fading and noise effects on the received data. The corresponding algorithms for the proposed LS-IPSO and LMMSE-IPSO channel estimators are described as follows:

Proposed LS-IPSO algorithm

- 1 Parameters Initialization: Particle size ($N_p = 50$), Number of Iterations ($T = 100$), inertia weight ($\omega = [0.4, 0.9]$) and acceleration constants ($C_1 = C_2 = 0.5$);
- 2 Estimate the LS channels according to (13) and uniformly randomly initialise each LS particle x_i , $\mathbf{H}_{LS}^1, \mathbf{H}_{LS}^2, \mathbf{H}_{LS}^3, \dots, \mathbf{H}_{LS}^n$ in the swarm;
- 3 **for** $k=1$ to T **do**
- 4 **for** $i=1$ to particle size ($N_p = 50$) **do**
- 5 Calculate the fitness of each particle and set P_{best} and G_{best} according to $(H - \mathbf{H}_{LS})/H$;
- 6 Calculate the adaptive inertia weight according to (20);
- 7 Calculate the velocity of each particle according to (18) using the new adaptive inertia weight ;

```

8       Update the position of particle  $x_i$  according to (19);
9       Calculate the fitness of  $x_i$  and update  $P_{best}$  and  $G_{best}$ ;
10      end for
11       $k++$ 
12      end for
13      Termination Stage: The final solution is the final  $G_{best}$ , selected based on the minimum
Mean Square Error (MSE) value of the LS channel estimate at the end of the 50th
iteration;
14      if termination==true;
15      end

```

Proposed LMMSE-IPSO algorithm

```

1      Parameters Initialization: Particle size ( $N_p = 50$ ), Number of Iterations ( $T = 100$ ), inertia
weight ( $\omega = [0.4, 0.9]$ ) and acceleration constants ( $C_1 = C_2 = 0.5$ );
2      Estimate the LMMSE channels according to (16) and uniformly randomly initialize each
LMMSE particle  $x_i$ ,  $H_{LMMSE}^1, H_{LMMSE}^2, H_{LMMSE}^3, \dots, H_{LMMSE}^n$  in the swarm;
3      for  $k=1$  to  $T$  do
4          for  $i=1$  to particle size ( $N_p = 50$ ) do
5              Calculate the fitness of each particle and set  $P_{best}$  and  $G_{best}$  according to  $(H_{LMMSE})/H$ ;
6              Calculate the adaptive inertia weight according to (20);
7              Calculate the velocity of each particle according to (18) using the new adaptive
inertia weight;
8              Update the position of particle  $x_i$  according to (19);
9              Calculate the fitness of  $x_i$  and update  $P_{best}$  and  $G_{best}$ ;
10             end for
11              $k++$ 
12             end for
13             Termination Stage: The final solution is the final  $G_{best}$ , selected based on the least Mean
Square Error (MSE) value of the LS channel estimate at the end of the 50th iteration;
14             if termination==true;
15             end

```


E. Complexity of the proposed algorithms

The complexity analysis is determined by counting the total number of complex additions and complex multiplications per iteration. For the PSO-inspired LS and LMMSE algorithms, the algorithm switches between PSO and LS, and, PSO and LMMSE, where the sources of complexity are as follows:

(i) Each n particles of \mathbf{H}_{LS} with l dimension require one complex ln multiplication, while n particles of \mathbf{H}_{LMMSE} with l dimension require three complex multiplications and one complex addition. Thus, for n particles of l dimensions each, $3ln$ complex multiplications and ln complex additions are required for the latter.

(ii) In computing the LS and LMMSE fitness functions, there are four complex multiplications and three complex additions. Thus, for n particles with l dimensions each, $4ln$ complex multiplications and $3ln$ complex additions are required.

(iii) In updating the particle's velocities, (18) that calculates the velocities of the particles per iteration per dimension within the search space, there are five complex multiplications and four complex additions. Since multiplication with the constant acceleration factors c_1 and c_2 values can easily be executed with the shift registers, they are ignored. Hence, for n particles of l dimensions each, $5ln$ complex multiplications and $4ln$ complex multiplications are required to calculate the velocity.

(iv) Updating the particle's position according to (19) requires one complex addition.

(v) In computing the MSE, the computations for the square of the error are ignored because the PSO algorithm compares the MSE resulting from all particles and takes the best one that accomplishes the least MSE, which could also be obtained by using mean error instead of MSE. Hence, there is $(N-1)n$ complex addition for the N size OFDM symbol.

In summary, the LS-PSO algorithm requires $10ln$ complex multiplications and $8ln+(N-1)n$ complex additions, so that its total complexity can be expressed as:

$$10ln+8ln+(N-1)n=18ln+(N-1)n \quad (21)$$

Similarly, the LMMSE-PSO algorithm requires $13ln$ complex multiplications and $9ln+(N-1)n$ complex additions, so its total complexity can be written as:

$$13ln+9ln+(N-1)n=22ln+(N-1)n \quad (22)$$

On the other hand, the IPSO-inspired LS and LMMSE algorithms introduced a few extra additions to the complexity of the PSO-inspired LS and LMMSE, since the improvement in the PSO comes only from the inertia weight. As the inertia weight is set as a constant value usually between 0.4 and 0.9, its complexity is taken care of by a shift register.

Nevertheless, computing the inertia weight using (20) results in one complex multiplication and one complex addition. Hence, the total complexity of LS-IPSO can be expressed as:

$$11\ln + 9\ln + (N - 1)n = 20\ln + (N - 1)n \quad (23)$$

Similarly, the complexity analysis of LMMSE-IPSO based on computing the inertia weight using (20) can be written as

$$14\ln + 10\ln + (N - 1)n = 24\ln + (N - 1)n \quad (24)$$

For clarity, Table V summarizes the computational complexity of the LS, LMMSE, LS-PSO, LMMSE-PSO, LS-IPSO and LMMSE-IPSO algorithms in terms of complex multiplications and additions.

TABLE V. COMPLEXITY ANALYSIS OF LS, LMMSE, LS-PSO, LMMSE-PSO, LS-IPSO AND LMMSE-IPSO

Algorithm	Multiplications	Additions
LS	N	0
LMMSE	$4N^3 + 18N - 12$	$4N^3 + 18N - 1$
LS-PSO	$10\ln$	$8\ln + (N - 1)$
LMMSE-PSO	$13\ln$	$9\ln + (N - 1)$
LS-IPSO	$11\ln$	$9\ln + (N - 1)$
LMMSE-IPSO	$14\ln$	$10\ln + (N - 1)$

IV. PERFORMANCE EVALUATION OF PROPOSED IPSO-BASED LS/LMMSE CHANNEL ESTIMATION ALGORITHMS

A. Simulation set-up

To evaluate the performance of the proposed channel estimation methods, we carried out the simulation of OFDM signal transmission using the BB-PLC System shown in Fig. 6. All simulations are performed using MATLAB/Simulink R2018b installed on a 64-bit Acer Aspire 5750 PC with Windows 10 Operating System, third-generation Intel(R)Core (TM) i3-2328M CPU @ 2.20GHz and 6 GB installed memory. Tables VI and VII listed the typical parameters used for the simulation.

At the transmitter, the binary information data to be transmitted are first modulated using an M-QAM modulator ($M = 8, 16, 32, 64$) and then encoded. For short data transmission, the serial data are converted to parallel data and then known pilots are multiplexed with the modulated to enable the proposed pilot-aided channel estimation in this paper. The block-type pilot arrangement[5], [21], is used since it is suitable for the frequency-selective LV BB-PLC channel considered in this work. This is in contrast to the comb-type pilot arrangement considered for fast-fading BB-PLC channels in [9]. Inverse Fast Fourier Transform (IFFT) is then applied to convert the frequency-domain signal into a time-domain signal. To prevent ISI, a cyclic prefix (also called guard interval), is added to each frame

by copying the appropriate part of the OFDM symbol and pre-pending it to the transmitted data/symbol.

After parallel-to-serial conversion, the time-domain signal is transmitted over the BB-PLC channel that is characterised by frequency offset, multipath, attenuation, frequency-selective fading and strong noise effects. These together are capable of reasonably degrading the signal quality during transmission. Specifically, the noise in the BB-PLC channel consists of coloured background noise, narrowband noise and the most disruptive impulsive noise[19], [20]. After transmission, the received data at the receiver side is first converted from serial data into parallel data before the cyclic prefix is removed.

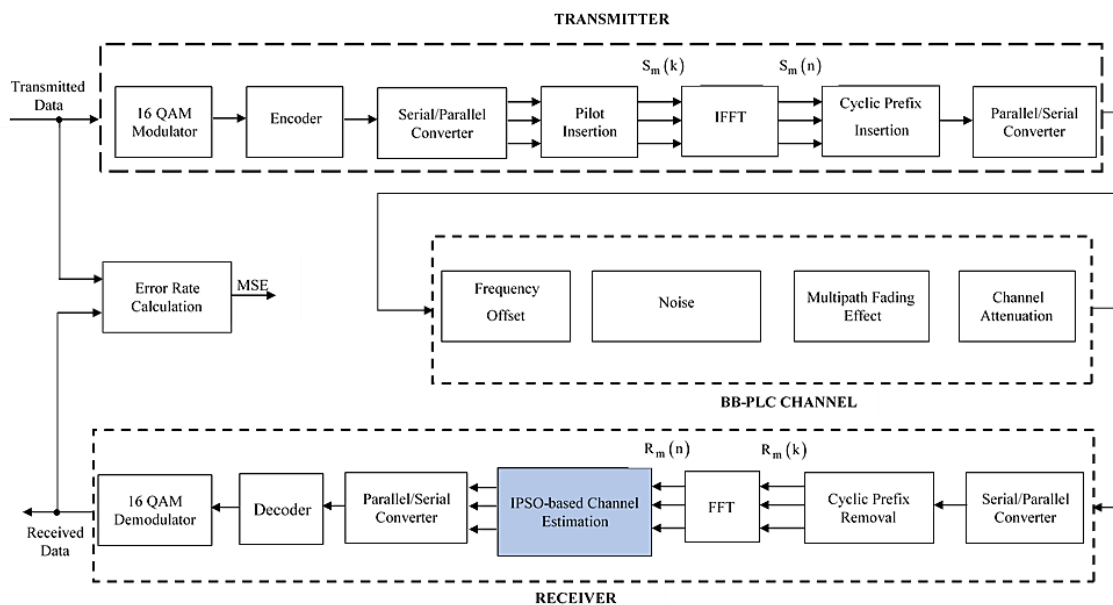


Fig. 6. Simulation setup of OFDM-based BB-PLC system with the proposed channel estimation method.

Next, a Fast Fourier Transform (FFT) is applied to convert the time-domain data stream into the frequency-domain data stream. The use of FFT avoids the complexity of the OFDM circuit as it reduces the number of filters and demodulators that may be required at the receiver. To recover the transmitted data bits with minimal MSE, the proposed IPSO-based LS/LMMSE channel estimation algorithm is then applied to estimate and remove the undesired interference effects introduced by the BB-PLC channel. Thereafter, the data is converted from parallel to serial form for decoding followed by demodulation using an M-QAM modulator ($M = 8, 16, 32, 64$) demodulator.

TABLE VI. OFDM-BASED BB-PLC SIMULATION PARAMETERS

Parameters	Specifications
FFT Interval (OFDM Samples)	512
FFT Size	64
PLC Frequency Range (MHz)	0-30
Interleaving (Pilot Arrangement)	Block-type
Pilot Energy	10
Cyclic Prefix Length	8
Cyclic Prefix Extension	5
Signal Constellation	QAM
Constellation Order	8, 16, 32, 64
BB-PLC multipath channel	BB-PLC multipath channel model, i.e., (1)
Number of Multipath	15
Attenuation Parameters	$k=1, a_1 = 0, a_1 = 7.8 \times 10^{-10}$ s/m
Normalized Frequency Offset	0.0625
Maximum Time Delay of Path i	$\tau_i = 6.94 \mu s$
Channel Noise Model	BB-PLC channel Noise model, i.e., (10)
Sampling Frequency (MHz)	320
Noise Bandwidth (MHz)	0 – 30
Mains Frequency (Hz)	50
Cycles needed for Noise	1
Sub-carrier Spacing (MHz)	5
Noise Samples Generated	16000

TABLE VII. IPSO PARAMETERS

Parameters	Rate
Problem dimension	128
Number of particles	50
Number of iterations	100
Inertia weight factor (ω)	$[0.4, 0.9], \omega_i(k)$
C_1	0.5
C_2	0.5

B. Performance evaluation results

In this section, we evaluate the performance evaluation results of our proposed PSO-inspired channel estimators. Notwithstanding its advantages, the PSO algorithm is generally vulnerable to local minima (i.e., local optima), where the particles become stagnant around the global minima and may be unable to reach the global minimum. It is therefore imperative to show that the optimisation of the fitness function for each proposed hybrid algorithm does not lead to issues of local optima. It is worthy to note that the proposed hybrid algorithms were executed independently, which means that each fitness function is updated separately for each proposed hybrid algorithm.

According to the principle of the traditional PSO algorithm, the optimised position of the swarm is based on continuous updates of the P_{best} and G_{best} values. In this case, the number of iterations for a given population may influence the final optimized position. Hence, to guarantee that no local optima ever occur when independently using each fitness function for each respective proposed hybrid algorithm, we first obtained in Fig. 7 a relationship between the P_{best} and G_{best} values for each fitness function versus the number of iterations. From Fig. 7(a) and (b), it can be seen that the G_{best} stabilises to a final solution for fewer iterations while the P_{best} continually explores the search space and approaches the G_{best} as the number of iterations increases. Indeed, the P_{best} stabilised at the same level as the G_{best} at the 100th iteration. This indicates that the optimisation process of the IPSO algorithm is optimum and devoid of local optima at the 100th iteration.

Hence, we set the maximum number of iterations to 100 for each hybrid algorithm proposed and applied in this work. It is fair to say that combining the IPSO algorithm with the LS algorithm as in Fig. 7(a) and the LMMSE algorithm as in Fig. 7(b) solves the problem of particle stagnancy. This is because the adaptive inertia weight used in the IPSO avoids the issue of local optima since particles with the minimum inertia weight will be responsible for fine search while particles with maximum inertia weight promote escape from the local optima.

According to (16), the performance of the LMMSE algorithm depends on the matrix size and SNR values. To verify this, in Fig. 8 (a), we obtained the MSE values as a function of SNR for different matrix sizes. Here, we use the performance of the LS estimator as a baseline for comparison. It can be seen that LS-5 and LMMSE-5 plots have a distinct performance from other curves (i.e., LMMSE-10, LMMSE-25, LMMSE-40 and LMMSE-60) for $I = N_p \times N_p$ matrix sizes where $N_p = 5, 10, 25, 40$ and 60 . This is because the MSE performance of the LMMSE channel estimator proportionally decreases with increasing matrix sizes, as shown in (16). In this case, increasing matrix sizes negates the expected MSE performance improvement for increasing SNR values. Hence, LS-5 and LMMSE-5 show superior performance compared to other curves.

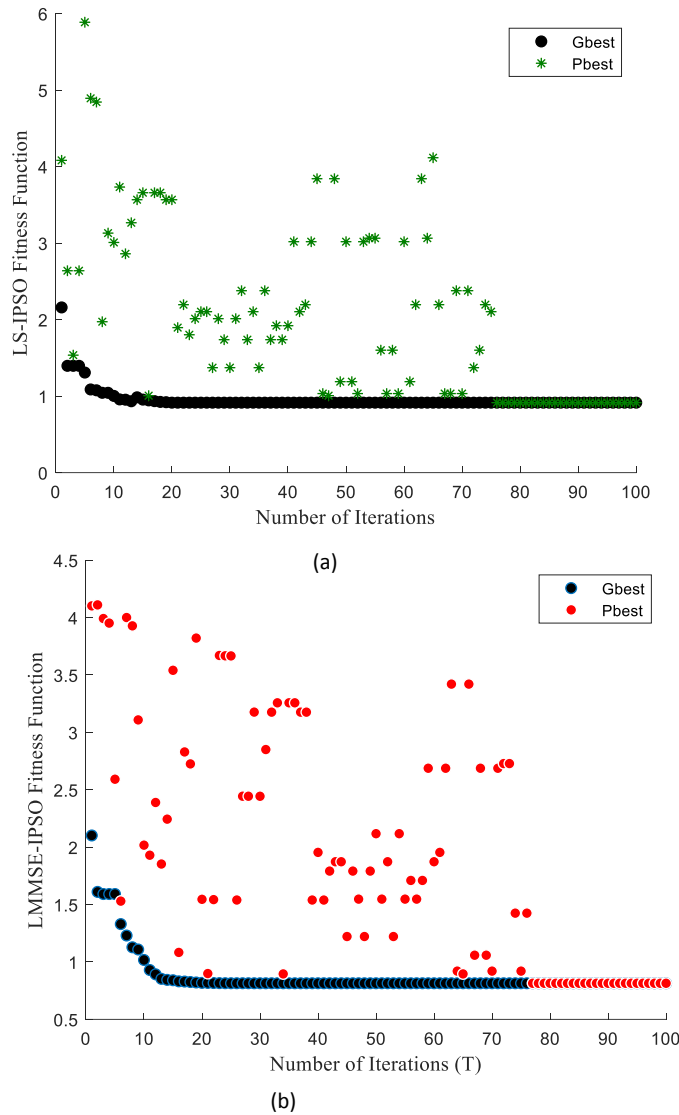


Fig. 7 P_{best} and G_{best} varied with the maximum iteration for (a) LS-IPSO fitness function (b) LMMSE-IPSO fitness function.

To illustrate the robustness of our proposed PSO-inspired channel estimators, in Fig. 8(b), we plot the MSE performance versus SNR for different matrix sizes. Compared to Fig. 8(a), it can be seen clearly that our proposed channel estimators still achieve the lowest acceptable MSE values for higher matrix sizes.

Next, the performance of the proposed PSO-inspired LS and LMMSE (i.e., PSO- and IPSO-based LS & LMMSE) and the LS and LMMSE algorithms are assessed in terms of MSE and computational complexity as a function of the SNR (Fig. 9). As can be seen from Fig. 9 (a), our proposed channel estimation methods outperform their respective conventional counterparts in terms of reduction in MSE values. In particular, at a lower SNR of 20 dB, our proposed PSO- and IPSO-based LMMSE and LS algorithms achieved approximately 7.5732×10^{-6} , 4.5228×10^{-4} , 8.3849×10^{-12} and 6.0157×10^{-9} MSE values respectively, compared to, 7.854×10^{-3} and 0.9945 MSE values for the conventional LMMSE and LS algorithms.

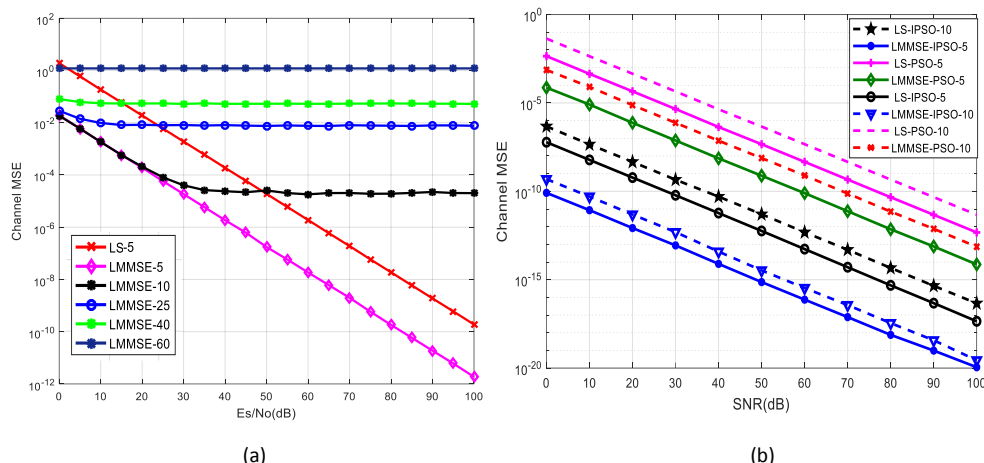


Fig. 8 MSE performance as a function of SNR and matrix size for (a) LMMSE estimator (b) Proposed PSO estimators.

At a higher SNR of 60 dB, the proposed PSO- and IPSO-based LMMSE and LS algorithms registered approximately 7.8913×10^{-11} , 4.6528×10^{-9} , 7.4541×10^{-17} and 5.4009×10^{-14} MSE values, compared to 5.7278×10^{-6} and 8.0168×10^{-4} for the conventional LMMSE and LS algorithms respectively. The results in Fig. 9(a) appear linear with respect to SNR in dB for different algorithms. Consequently, using the curve fitting in MATLAB to fit a linear relationship between MSE and SNR for the LMMSE-IPSO algorithm, we can obtain the equation:

$$\text{MSE} = -3.675 \times 10^{-7} (\text{SNR}) + 2.59 \times 10^{-5} \quad (25)$$

These results obtained for a higher SNR demonstrated the superiority of our proposed algorithms over their traditional implementations and would guarantee efficient data demodulation at the receiver with or without minimal errors. This is because the closer the value of the MSE of a particular estimator to zero, the lesser the error and the better the performance of the channel estimator in retrieving data sent over the BB-PLC channel for smart grid applications such as smart metering in power transmission and distribution networks.

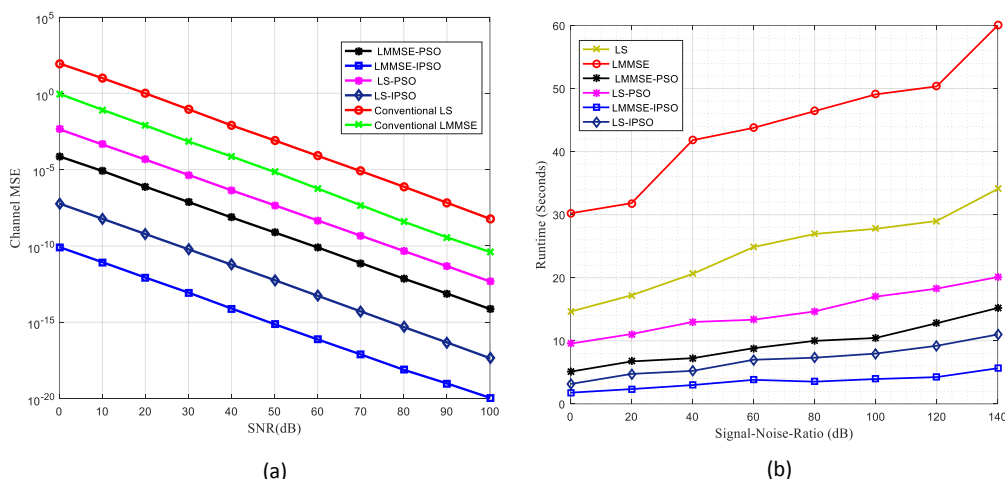


Fig. 9. (a) MSE Performance as a function of SNR for proposed channel estimators with respect to conventional LS and LMMSE channel estimators, (b) Complexity Evaluation of Proposed Channel Estimators in terms of Computational Runtime vs SNR values.

As can be seen clearly from Fig. 9 (b), the computational complexity of the proposed algorithms is much lower compared to the traditional algorithms. In particular, at 100 dB SNR, the proposed PSO- and IPSO-based LMMSE and LS achieved a computational runtime of 10.452s, 16.997s, 3.939s and 7.973s respectively. In contrast, the conventional LS and LMMSE estimators used about 28.00s and 49.071s computational runtime, respectively at 100dB SNR. In effect, the proposed LMMSE-IPSO and LS-IPSO about achieved about 91.97% and 71.53% savings in terms of computational runtime, respectively over their conventional counterparts. This result confirms the prediction of the complexity analysis carried out in section E.

Furthermore, we test the robustness of our proposed algorithms for different QAM constellation orders (8-QAM, 16-QAM, 32-QAM and 64-QAM), since higher transmission data, rates can be accomplished with the use of higher-order QAMs without necessarily increasing the bandwidth of the OFDM-based BB-PLC system. In this case, it can be expected that performance will degrade woefully for higher modulation order M-ary QAM formats. Therefore, in Fig. 10, we obtained and plot the MSE performance versus SNR of our proposed algorithms for 8-QAM, 16-QAM, 32-QAM and 64-QAM constellations. As can be seen from Fig. 10, the MSE performance deteriorates with increasing order of QAM formats due to reduced Euclidean distances between the constellation points.

As can be seen from Fig. 10, the MSE performance deteriorates with increasing order of QAM formats due to reduced Euclidean distances between the constellation points. In all cases, our proposed channel estimators still show superior MSE performance within an acceptable MSE limit, compared to the conventional LS and LMMSE estimators.

Previous results have established the superior performance and lower complexity of our proposed hybrid PSO-inspired LS and LMMSE algorithms in comparison with the traditional LS and LMMSE channel estimators. Nevertheless, it is equally important to compare with some recent state-of-the-art works to show the effectiveness and novelty of our proposed channel estimators. For this reason, in Fig. 11, we compared our work with the matched filtering and dynamic peak-based threshold estimation-partial transmit sequence (DPTE-PTS) techniques introduced in [2] and [25] respectively. As can be seen in Fig. 11, our proposed schemes IPSO-based LS and LMMSE estimators outperform the schemes in [2]and [25]. For instance, at a lower 20 dB SNR, the proposed IPSO-based LMMSE and LS algorithms attained nearly 8.3849×10^{-12} and 6.0157×10^{-9} MSE values, compared to, 9.35×10^{-8} and 7.854×10^{-7} MSE values for the matched filter and DPTE-PTS algorithms, respectively. However, the schemes in [2] and [25] show superior performance over the proposed PSO-inspired LS and LMMSE estimators. Specifically, the proposed PSO-based LMMSE and LS algorithms attained nearly 7.5732×10^{-6} and 4.5228×10^{-4} MSE values, compared to the MSE values obtained for the state-of-the-art works [2][25], respectively.

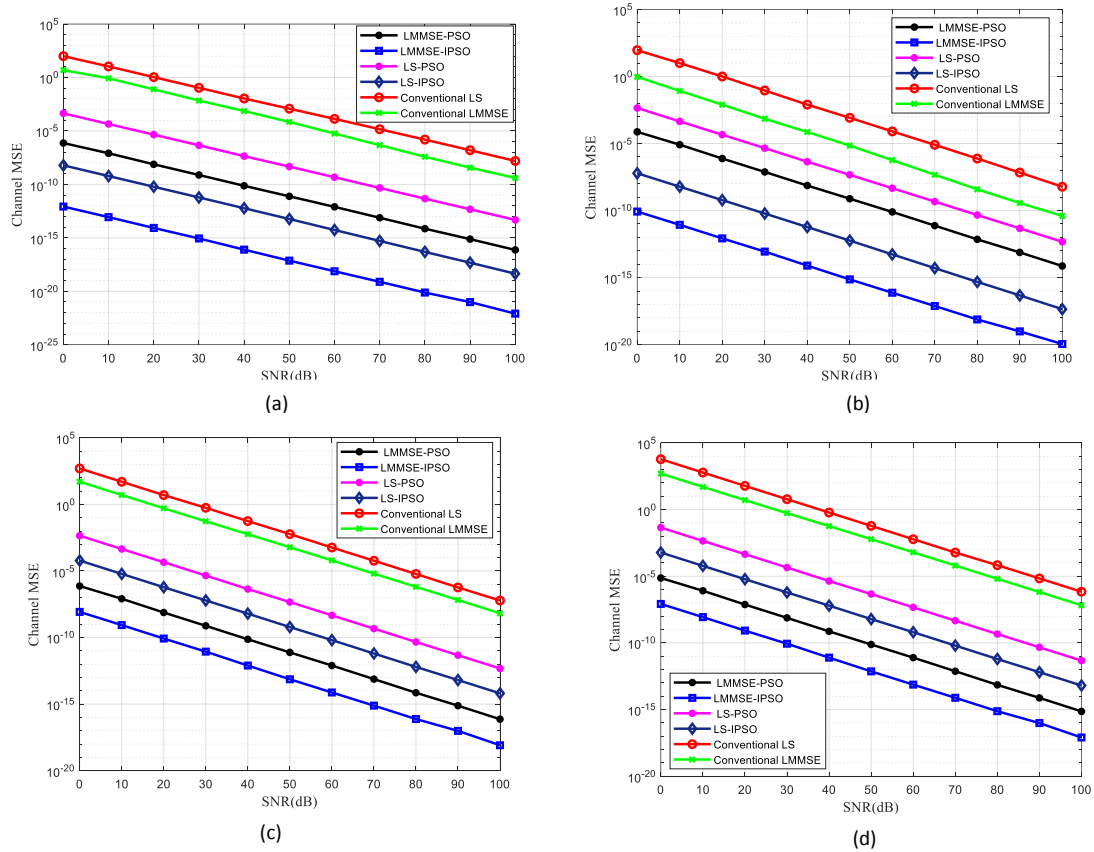


Fig. 10 MSE performance of proposed channel estimators using (a) 8-QAM, (b) 16-QAM, (c) 32-QAM and (d) 64-QAM constellations.

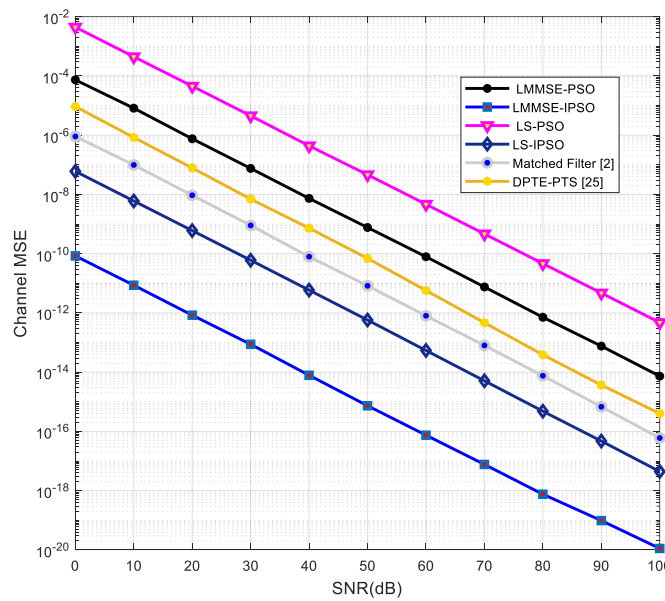


Fig. 11. MSE performance of proposed channel estimators with respect to state-of-the-art estimators in terms of SNR.

V. RELATED WORKS AND DISCUSSIONS

Several channel estimation techniques have been reported in the literature for OFDM-based Low-Voltage BB-PLC systems. A blind channel estimation technique based on the PSO algorithm was developed in [7] to combat impulsive noise in the PLC system. The authors show that the proposed blind PSO approach improved system performance but deteriorates at higher SNRs. In [9], an enhanced LMMSE channel estimation scheme was proposed that uses some taps as the channel energy and considered the remaining taps as the noise variance. Although the proposed LMMSE channel estimator improved the system performance, the MSE/BER performance was minimal when more taps were considered for the noise energy [9]. In addition, the authors did not consider computational complexity. In [26], modified compressed sensing based on Sparse Bayesian Learning (SBL) was proposed, which improved the noise rejection capability by estimating the sparsity and impulsive noise of the PLC channel. Nevertheless, the computational complexity of the proposed SBL method was high. Deterministic and random Maximum-Likelihood (ML) channel estimators for the PLC system were advanced in [8]. These ML estimators improve upon system performance in terms of MSE reduction, but at the expense of higher complexities. A Turbo Equalizer for the PLC system was proposed in [27] which showed marginal performance in terms of MSE reduction for all SNR values and greatly reduced the computational complexity. A matched filter for an OFDM-based PLC system was investigated in [2] for guaranteed low computational complexity and MSE reduction capability, but such a filter is impracticable. In [25], Dynamic Peak-Based Threshold Estimation is combined with Partial Transmit Sequence (DPTE-PTS) technique to suppress impulsive noise in the PLC system. The MSE reduction performance of this proposed technique was peripheral but the authors did not consider the computational complexity. It is worth mentioning that several of these channel equalization techniques attempted to find the optimal MSE reduction or noise rejection capability of the channel at low computational complexity. However, their implementations reveal that either the MSE performance improvement is minimal or the computational load complexity is high.

In this work, we appended the traditional PSO and our improved PSO (i.e., IPSO) to the conventional LS and LMMSE channel estimation approach to advance four new channel estimators (i.e., LS-PSO, LMMSE-PSO, LS-IPSO and LMMSE-IPSO). Contrary to the blind PSO used in [7], the PSO applied in this work is based on pilot symbols. Compared to the channel estimators discussed previously, our proposed techniques showed superior performance in terms of MSE reduction with low computational complexity. This show that our channel estimation techniques are effective for OFDM-based PLC systems and offer a better trade-off between MSE reduction and computational load complexity. For convenience, a comparison between these different channel estimation algorithms for OFDM-based PLC systems is illustrated in Table VIII.

TABLE VIII. COMPARISON OF DIFFERENT OFDM-BASED PLC CHANNEL ESTIMATION TECHNIQUES

Channel Estimation Method	MSE Reduction Performance	Computational Complexity
PSO-based Blind Channel Estimation [7]	Low	-
Improved LMMSE [9]	Low	-
Compressed Sensing [26]	Medium	High
Maximum Likelihood Estimators [8]	Medium	High
Turbo Equalizer [27]	Low	Medium
Matched Filter [2]	Medium	Low
DPTE-PTS [25]	Low	-
LS-PSO, LMMSE-PSO, LS-IPSO, LMMSE-IPSO	High	Low

VI. CONCLUSION

In this paper, we have proposed pilot-assisted PSO-inspired LS and LMMSE channel equalization methods for low-voltage broadband OFDM-based PLC systems. For the proposed channel estimators, we applied the traditional PSO algorithm and its proposed improved version to optimize the performance of the basic LS and LMMSE channel estimation algorithms respectively. While the PSO algorithm improves the noise rejection capability of the basic LS algorithm, it reduces the computational complexity of the LMMSE algorithm. Results of extensive numerical simulations conducted using four different M-QAM formats ($M = 8, 16, 32, 64$) to evaluate the feasibility of the proposed algorithms show that our proposed PSO-inspired LS and LMMSE estimation methods offer better performance, at least for the system parameters studied in this work, compared to the traditional implementation of LS and LMMSE algorithms and few other state-of-the-art works.

REFERENCES

- [1] G. López, J. Matanza, D. De La Vega, M. Castro, A. Arrinda, J. I. Moreno and A. Sendin, "The role of power line communications in the smart grid revisited: Applications, challenges, and research initiatives," *IEEE Access*, vol. 7, pp. 117346–117368, 2019, doi: 10.1109/ACCESS.2019.2928391.
- [2] M. Colombo, A. Hernandez, and J. Urena, "Low-Complexity Joint Time Synchronization and Channel Estimation for OFDM-Based PLC Systems," *IEEE Access*, vol. 7, pp. 121446–121456, 2019, doi: 10.1109/access.2019.2937472.
- [3] A. Llano, D. De La Vega, I. Angulo, and L. Marron, "Impact of Channel Disturbances on Current Narrowband Power Line Communications and Lessons to Be Learnt for the Future Technologies," *IEEE Access*, vol. 7, pp. 83797–83811, 2019, doi: 10.1109/ACCESS.2019.2924806.
- [4] D. Bueche, P. Corlay, M. Gazalet, and F. X. Coudoux, "A method for analyzing the performance of comb-type pilot-aided channel estimation in power line communications," *IEEE Trans. Consum. Electron.*, vol. 54, no. 3, pp. 1074–1081, 2008, doi: 10.1109/TCE.2008.4637590.
- [5] M. Chen, S. You, Y. Wang, Z. Wang, S. Bian, H. Chen, J. Ding, H. Wu, R. Shi, S. Zhou and J. Chen., "Performance analysis of pilot-based OFDM channel estimation for hybrid PLC&VLC system," in *ICOON 2016 - 2016 15th International Conference on Optical Communications and Networks*, 2017, pp. 1–3, doi: 10.1109/ICOON.2016.7875704.

- [6] A. Bogdanović, M. Bažant, “Improved Least Square Channel Estimation Algorithm for OFDM-based Communication over Power Lines,” *Mediterr. J. Comput. Networks*, vol. 10, no. 2, pp. 1–7, 2014.
- [7] G. A. Laguna-Sanchez, R. Barron-Fernandez, “Blind Channel Estimation for Power Line Communications by a PSO-inspired Algorithm,” in *IEEE Latin-American Conference on Communications (LATINCOM)*, pp. 1–6, 2009.
- [8] D. Shrestha, X. Mestre, and M. Payaró, “On channel estimation for power line communication systems in the presence of impulsive noise R,” *Comput. Electr. Eng.*, vol. 72, pp. 406–419, 2018, doi: 10.1016/j.compeleceng.2018.10.006.
- [9] X. D. Sheng, L. He, S. Pu, G. X. and Guo, “An Improved LMMSE Channel Estimation Algorithm for OFDM-based Low Voltage Power Line,” in *EEE Transportation Electrification Conference and Expo, Asia-Pacific (ITEC Asia-Pacific)*, pp. 1–5, 2017.
- [10] Y. Zhang, K. Liang, Y. He, Y. Wu, X. Hu, and L. Sun, “The Channel Compressive Sensing Estimation for Power Line Based on OMP Algorithm,” *J. Electr. Comput. Eng.*, vol. 2017, pp. 1–8, 2017, doi: 10.1155/2017/2483586.
- [11] F. Pancaldi, F. Gianaroli, and G. M. Vitetta, “Equalization of narrowband indoor powerline channels for high data rate OFDM communications,” *IEEE Trans. Smart Grid*, vol. 9, no. 1, pp. 78–87, 2018, doi: 10.1109/TSG.2016.2545108.
- [12] Z. Peiling. and Z. Hongxin, “Channel estimation in OFDM power line communication based on pilots and particle filtering,” in *Chinese Control and Decision Conference (CCDC)*, 2016, pp. 6941–6946, doi: 10.1109/CCDC.2016.7532249.
- [13] N. Shlezinger, K. Todros, and R. Dabora, “Adaptive Filtering Based on Time-Averaged MSE for Cyclostationary Signals,” *IEEE Trans. Commun.*, vol. 65, no. 4, pp. 1746–1761, 2017, doi: 10.1109/TCOMM.2017.2655526.
- [14] S. M. Curuk, “Channel Estimation for OFDM Systems in Power Line Communication,” in *IEEE Signal Processing and Communications Applications Conference (SIU)*, pp. 1–4, 2015.
- [15] M. Asadpour, “A Novel Channel Estimation Method for Power Line Communications,” *Commun. Appl. Electron.*, vol. 7, no. 10, pp. 21–27, 2017.
- [16] M. Zimmermann and K. Dostert, “Analysis and modeling of impulsive noise in broad-band powerline communications,” *IEEE Trans. Electromagn. Compat.*, vol. 44, no. 1, pp. 249–258, 2002, doi: 10.1109/15.990732.
- [17] M. Zimmermann and K. Dostert, “A Multipath Model for the Power Line Channel,” *IEEE Trans. Commun.*, vol. 50, no. 4, pp. 553–559, 2002.
- [18] M. Zimmermann and K. Dostert, “A multi-path signal propagation model for the power line channel in the high frequency range,” in *3rd International Symposium on Power-line Communications*, vol. 30, no. 1, pp. 45–51, 1999.
- [19] K. Yan, H. Zhang, and H. C. Wu, “Robust multipath channel estimation in the presence of impulsive noise,” *IET Commun.*, vol. 12, no. 2, pp. 228–235, 2018, doi: 10.1049/iet-com.2017.0374.
- [20] B. Rajkumarsingh and B. Sokappadu, “Noise Measurement and Analysis in a Power Line Communication Channel,” in *International Conference on Emerging Trends in Electrical, Electronic and Communications Engineering*, pp. 81–93, 2017.
- [21] L. Lampe, A. M. Tonello, and T. G. Swart, *Power Line Communications: Principles, Standards and Applications from Multimedia to Smart Grid*, 2nd ed. New Jersey, U.S.A: John Wiley and Sons Ltd, 2016.
- [22] S. Iwata, Y. Fukuyama, T. Jintsugawa, H. Fujimoto, and T. Matsui, “Dependable Multi-population Different Evolutionary Particle Swarm Optimization for Distribution State Estimation using Correntropy,” *IFAC-PapersOnLine*, vol. 51, no. 28, pp. 179–184, 2018, doi: 10.1016/j.ifacol.2018.11.698.
- [23] M. G. S. Wicaksana, L. M. Putranto, F. Waskito and M. Yasirroni, “Optimal Placement and Sizing of PV as DG for Losses Minimization Using PSO Algorithm: a Case in Purworejo Area,” in *International Conference on Sustainable Energy Engineering and Application (ICSEEA)*, pp. 1–6, 2020, doi: 10.1109/ICSEEA50711.2020.9306134.
- [24] M. Li, H. Chen, X. Wang, N. Zhong, and S. Lu, “An Improved Particle Swarm Optimization Algorithm with

- Adaptive Inertia Weights,” *Int. J. Inf. Technol. Decis. Mak.*, vol. 18, no. 3, pp. 833–866, 2019.
- [25] J. Ding, H. Xu, D. Huang, X. Cheng, X. Yang, C. Liu and Y. Wang, “A Channel Estimation Algorithm for Impulse Noise Suppression in PLC System,” in *International Conference on Communication Technology Proceedings, ICCT*, 2020, pp. 34–38, doi: 10.1109/ICCT50939.2020.9295709.
- [26] X. Lv and Y. Li, “Joint channel estimation and impulsive noise mitigation for power line communications,” in *2018 24th Asia-Pacific Conference on Communications, APCC 2018*, 2019, pp. 576–579, doi: 10.1109/APCC.2018.8633486.
- [27] A. Chehri, “A Low Complexity Turbo Equalizer for Power-Line Communication with Applications to Smart Grid Networks,” in *2019 IEEE International Symposium on Power Line Communications and its Applications (ISPLC)*, pp. 1–6, 2019, doi: 10.1109/ISPLC.2019.8693313.